THE INFLUENCE OF WATER ABSORPTION ON THE DAMAGE MECHANISM OF UNIDIRECTIONAL AND 2D WOVEN CFRP

Faisel Almudaihesh[1], Stephen Grigg[1], Rhys Pullin[1], Karen Holford[1], and Mark Eaton[1]

[1]Tribology and Performance of Machines, Structures and Materials Group, School of Engineering, Cardiff University, Queen's Buildings, The Parade, Cardiff CF24 3AA, United Kingdom
Email: almudaiheshFS@cardiff.ac.uk
Website: https://www.cardiff.ac.uk/engineering

Keywords: Carbon-polymer matrix composites, Fibre architecture, Water absorption, Damage mechanism, and Acoustic emission.

ABSTRACT

This study presents the influence of water exposure on unidirectional, plain weave, and twill weave CFRP particularly in the interfacial region. Specimens were exposed to 70°C water for 40 days and tested using the short-beam method to evaluate their interlaminar strength. This was conducted with the use of Acoustic Emission and Video Strain Gauge (an optical strain measurement). Scanning Electron Microscope was also used in this study. Results show weight increase of specimens due to water exposure by 1%, 0.94%, and 0.99% for unidirectional, plain and, twill, respectively. Furthermore, significant reductions in the short-beam strengths were observed for aged specimens. Acoustic emission showed promising initial results which can help to distinguish between the different damage mechanisms of aged and unaged specimens further enhancing the understanding of crack formation prior to final interlaminar failure. In addition, matrix cracking, fibre/fibre detachment, and fibre/matrix cracks were observed in the Scanning Electron Microscope results.

1 INTRODUCTION

The use of CFRP laminates are significantly increasing in the aerospace, automotive, and marine industries particularly in safety critical primary structures due to their excellent fatigue and corrosion resistance properties compared with metallic materials [1]. CFRP prepregs consist of reinforcing carbon fibres distributed in an epoxy resin which can be in the form of unidirectional or a range of woven architectures in both biaxial and triaxial forms. Prepregs are particularly attractive due to their precisely controlled resin distribution [2,3]. Many CFRP structures are at high risk of structural and environmental impacts whilst in operation which can significantly influence their overall performance [4]. This study aims to evaluate the influence of water absorption on the interlaminar damage mechanism with the use of Acoustic Emission (AE), Video Strain Gauge (VSG), and Scanning Electron Microscope (SEM).

AE is the spontaneous release of energy caused by the growth of damage; this energy propagates as an ultrasonic stress wave. By monitoring a structure for AE, it is possible to identify the initiation, and track the growth of damage [5]. Studies have been conducted to further understand the effect of moisture absorption on the mechanical properties and their failure modes. AE has become an essential test technique that can monitor the damage behaviour and gain deep insight into the failure mechanisms and damage evolution behaviour of composites under hygrothermal environments [6,7]. AE is used in this study to distinguish the damage mechanism between unaged and aged CFRP specimens by acquiring different parameters from the AE waveforms where Figure 2 summarises the acquired parameters in this study [8]. The threshold is a pre-set voltage level that a received AE signal must exceed to be detected and processed.

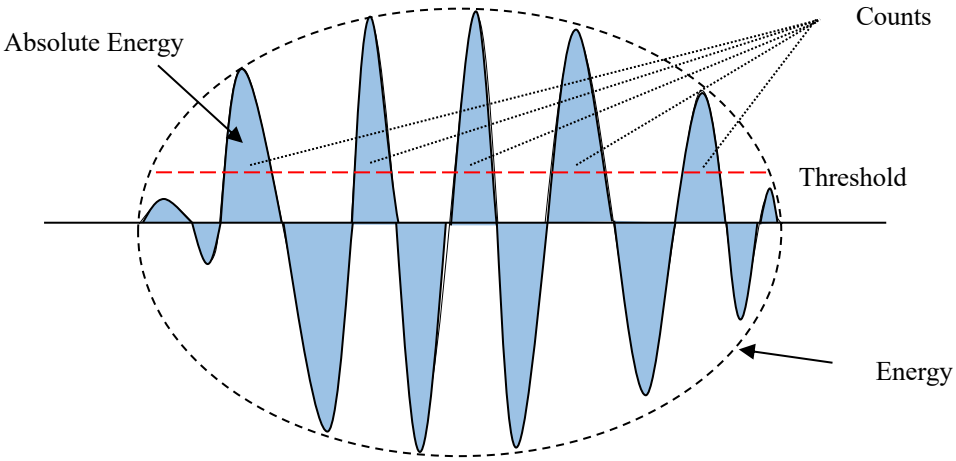

Figure 1: AE Waveform features.

The terms can be defined as [8]:
Energy: integral of the rectified voltage signal over the duration of the AE waveform.
Counts: the AE signal excursions over the AE threshold.
Absolute Energy: a true energy measure of the AE waveform. It is a six-byte value whose units are aJ "attoJoules".

The VSG is an optical strain measurement technique that exploits a sub-pixel pattern recognition algorithms which enable ultra-high resolution measurements. The tool allows the use of a shear sensor that monitors the shear strain based on the shear angle of a rectangular region as illustrated in Figure 1 [9].

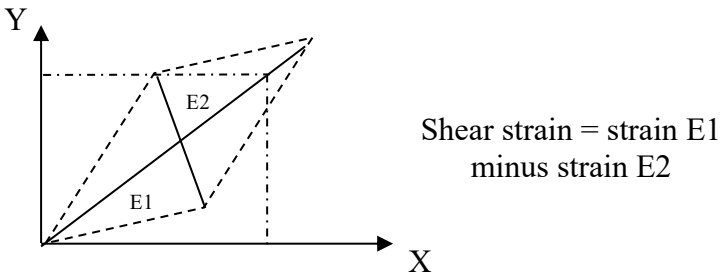

Figure 2: VSG shear strain measurements.

2 METHODS

2.1 Materials

Three versions of CFRP prepreg were used in this work manufactured by SK chemicals using Skyflex K51 Epoxy resin. The specification of each prepreg variant used were: high strength Pyrofil TR50S unidirectional carbon fibre, 200gsm with 33% resin content and sizing content of 1%; high strength Pyrofil TR30S 3k plain weave, 198gsm with 40% resin content and sizing content of 1.2%; and 2x2 twill high strength Pyrofil TR30S 3k twill weave, 198gsm with 40% resin content and sizing content of 1.2%. Large panels were manufactured and cut into the desired specimen dimensions. Thirty plies with stacking sequences of $[0/90]_{15}$ and $[(0/90)]_{30}$ for unidirectional (nominally 5.8 mm thick) and woven (nominally 6.4 mm thick) were used, respectively. The stacking sequences were selected to create identical distribution of fibre directions between unidirectional and woven specimens for comparison purposes. Debulking operations were applied when making the specimens panels due to their large thicknesses. The process applied vacuum pressure at room temperature for

five minutes following layup of five plies, until the final thickness was achieved. All materials were cured with the same cure cycle as recommended by the materials supplier, using an autoclave under two dwells: 30 minutes at 80°C temperature and 5 bar pressure followed by 60 minutes at 125°C temperature and 5 bar pressure. The matrix volume content was obtained for all specimens in accordance with ASTM D3171 method 1 procedure A [10]. This was carried out by using 60ml nitric acid for each specimen at 80°C for six hours. The carbon fibres were then filtered into pre-weighed sintered glass filters under a vacuum of better than 17 kPa. The carbon fibres were cleaned with water at least three times and a final acetone wash followed by one hour oven drying at 100°C. They were then left to cool to room temperature. The weight was then recorded to the nearest 0.0001g using Sartorius LA310S analytical balance.

2.2 Water Absorption and Interlaminar Strength

Water absorption testing was carried out using non-ambient moisture conditioning in a mineral water immersion tank at a prescribed constant temperature of 70°C for a fixed-time period of 40 days, in accordance with ASTM D5229 procedure BWFF [11]. The water used featured typical contents values of 48.5mg/l calcium, 5.2mg/l magnesium, 14.0mg/l sodium, 0.8mg/l potassium, 148.0mg/l bicarbonate, 10.7mg/l chloride, 27.6mg/l sulphate, and 4.0mg/l nitrate. The specimen water content was determined as a percentage change using (Eq. 1) [11].

$$\textit{Mass percentage change, \%} = ((W_i - W_o) / W_o)*100 \quad (1)$$

Where W_i is the weight of the specimen at each point of record during the experiment, and W_o is the initial dry weight of the specimen before any contact with water.

The interlamiar strength characterisation was fulfilled by employing the short-beam strength test using a three-point bending (3PB) configuration in a Zwick Roell Z050 load machine with 50kN load cell. The loading nose was 6mm in diameter, the supports were 3mm in diameter, the span distance was 24mm, and the speed of testing was at a crosshead rate of 1mm/min in accordance with ASTM D2344 [12]. A minimum of ten specimens were prepared for each fibre architecture (five for dry and five for water-immersed). All specimens were 36mm by 12mm. This test configuration was set to promote interlamianr shear failure mode. Other specimen thicknesses trialled led to failure modes that are not representative for interlaminar shear aimed for this study (as described in ASTM D2344 [12]). For instance, flexure failure in compression or tension was found in thinner specimens. Additionally, inelastic deformation was reported in thicker specimens. The short-beam strength was calculated using (Eq. 2) [12].

$$F_{sbs} = 0.75*P_m/b*h \quad (2)$$

Where F_{sbs} is the short beam strength (MPa), P_m is the maximum load observed during the test (N), b is the measured specimen width (mm), and h is the measured specimen thickness (mm).

2.3 AE and VSG

AE signals were recorded with a MISTRAS system. The system consisted of a preamplifier set to 40 dB, a PICO sensor, and connected to a MISTRAS PCI2 AE system with AEwin software. The same sensor was used in all 3PB specimens that have been used for the AE analysis. The sensor was mounted to the top surface of the specimen (as shown in Figure 3) using super glued which provides physical attachment and acoustic coupling.

An Imetrum VSG system was used in this study to measure the shear strain of all specimens. A 5MPixel IMT-CAM028 camera with IMT-LENS-MT043 material test lenses was used with a field of view of 40x36 mm. A suitable speckle pattern was applied to all specimens that have been used for the video strain gauge analysis, in-line with Imetrum guidance. This was achieved by spraying the specimens with a light dusting of matt white spray paint followed by a light dusting of matt black paint. This produces a pattern with many light, dark and grey areas suitable for precise target tracking.

The shear strain gauges were placed symmetrically about the central loading nose and within the support rollers, as illustrated in Figure 3, to monitor the regions of greatest shear displacement.

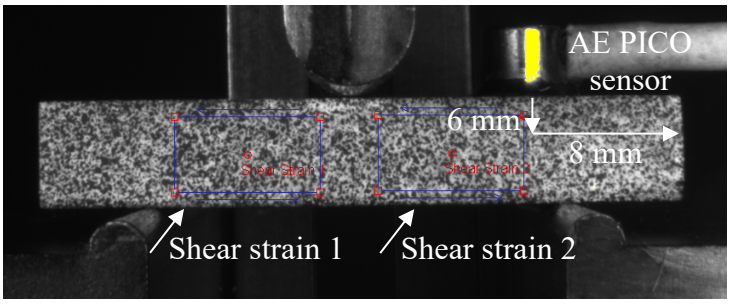

Figure 3: 3PB, AE, and VSG set-up.

2.4 SEM

ZEISS Sigma HD was adopted to impair high imaging quality and scrutinise the ageing effects at micro-structural level under different magnification. Specimens with 3mm by 12mm cut from the same panel as the 3PB specimens. These specimens were immersed in water with the 3PB specimens. Prior to SEM imaging, all specimens were oven dried at 50°C for 24 hours. The specimens were then metal coated with 10-15 nm with 90% gold/10% palladium layer to enhance the detection resolution by improving the conductivity of the material's surface avoiding charging effects. The data were analysed using ZEISS SmartSEM software.

3 RESULTS AND DISCUSION

Figure 4 presents the average weight increase for all specimens prior to the short-beam strength testing. A slight increase in weight gain was observed in UD specimens compared with woven specimens. This suggests that several factors can affect the water ingress mechanism. In this case, the uniformity of the fibres which can influence the diffusion rate along the fibres direction where the weave pattern "crimp" can contribute in slowing down the penetration rate. In addition, the differences noted on the sizing level between UD and woven of the materials used in this study can have a significant influence on the fibre/matrix interface after aging as further demonstrated with the SEM figures in this study, which therefore influences on the weight increase percentages observed.

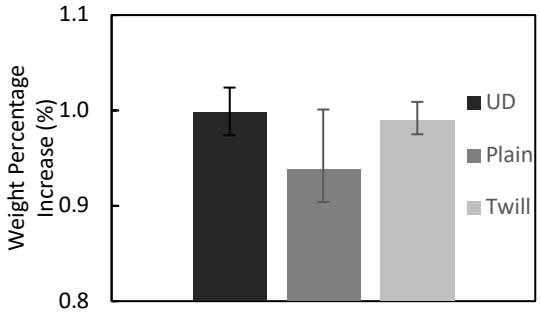

Figure 4: Weight change after 40 days of water exposure.

Figure 5 presents the short beam stress versus shear strain obtained from the VSG (red line) and the AE Energy (black markers). One representative example is shown in this report for each category. The short-beam strength of wet UD samples reduced by 8.38% compared with their dry equivalent. The wet plain and twill weave samples exhibited a reduction in short-beam strength of 6.74%, and 6.15% compared with their dry equivalents. The reduction in short beam strengths can be correlated to the effected matrix due to degradation where several cracks were observed from the SEM results shown in Figures 6-8 as well as the condition of the interface illustrated in Figure 9.

The presented AE data show that a number of high energy signals are recorded prior to failure in the dry specimens, whereas, very little high energy activity is seen prior to failure in the wet samples. The higher energy signals observed in the dry samples are thought to correlate to micro cracking in brittle matrix and initiation of fibre matrix debonding. In the case of the wet samples the matrix is expected to have plasticised and increased ductility, therefore reducing the sharp brittle release of acoustic energy. It is also evident from Figure 9 that significant microcracking and fibre matrix debonding has been induced by the hygrothermal degradation prior to loading and hence less emissions can be expected from these mechanisms during the 3PB testing. The absolute energy was found to show similar trends of the energy with respect to the differences in the values. Furthermore, higher cumulative counts were observed in all dry specimens at the point of maximum short-beam strength compared with their wet equivalents, as presented in Table 1. This is expected as dry specimens have the capability to withstand higher residual stresses prior to final stage of failure as well as the matrix being more brittle in its dry condition, which therefore increases the amount of AE signals.

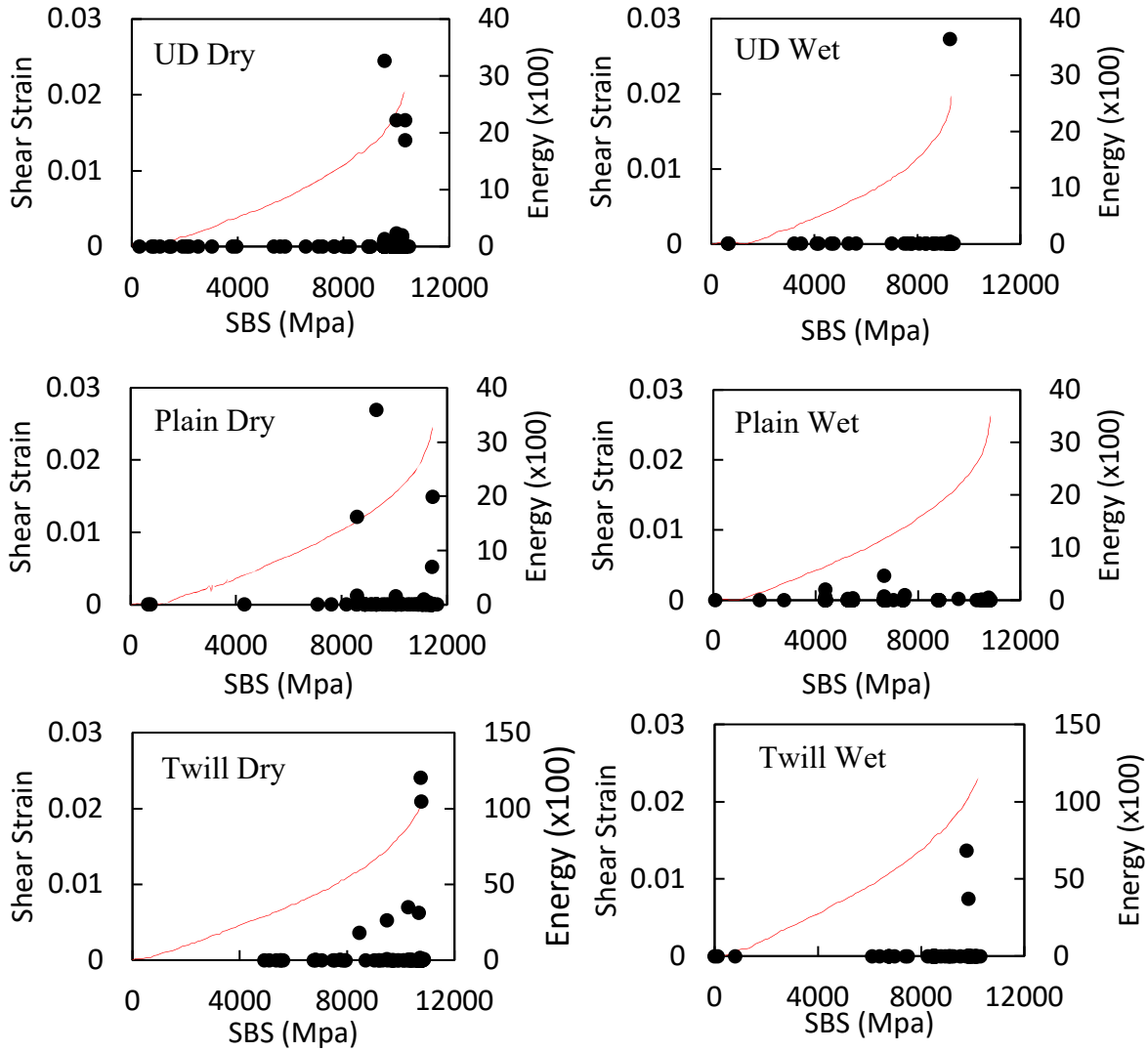

Figure 5: Short-beam strength, Energy from AE, and shear strain from VSG for all specimens.

Sample Condition	UD	Plain	Twill
Dry	6239	18231	3231
Wet	2729	3794	1472

Table 1: Average cumulative counts at maximum short-beam strength.

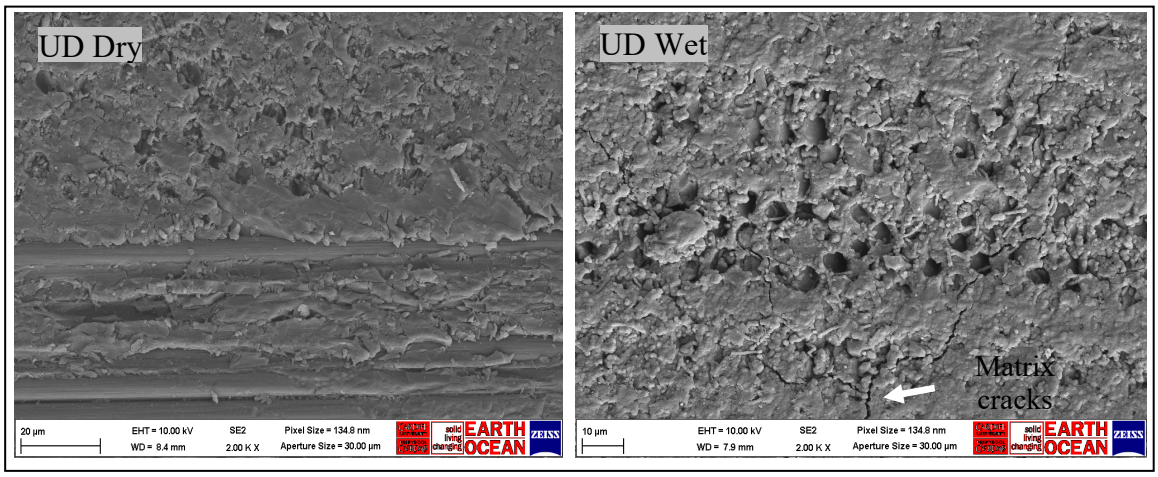

Figure 6: SEM for UD.

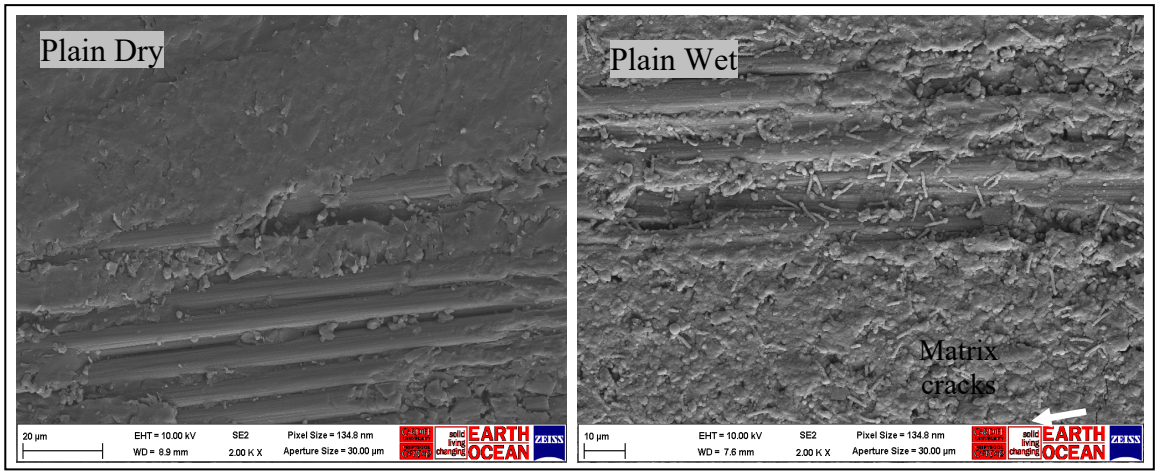

Figure 7: SEM for plain.

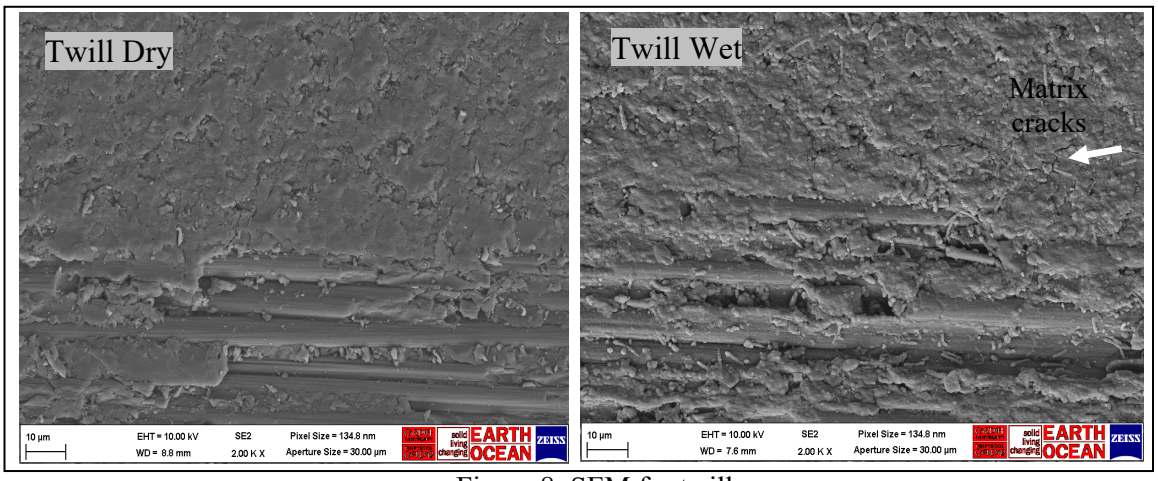

Figure 8: SEM for twill

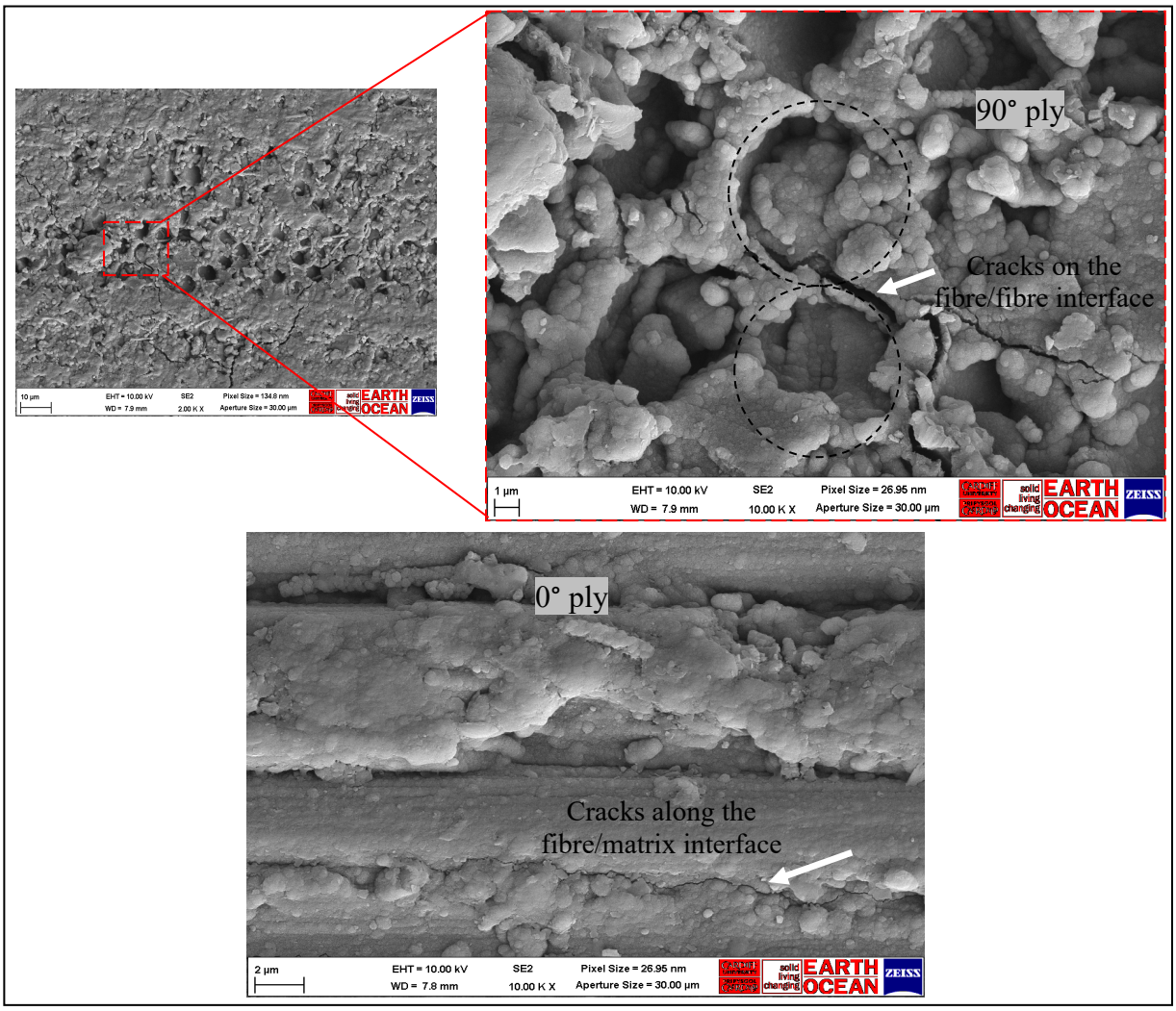

Figure 9: SEM for 90° and 0° plies of a wet UD specimen.

4 CONCLUSIONS

Moisture environments can affect the performance of CFRP in real life applications. This study shows the reduction of the interlaminar strength obtained after water exposure of CFRP specimens with different fibre architecture. The use of AE is a helpful tool that can be used to monitor crack formation of all specimens prior to final failure. AE can also be used to further inform researches that study the fibre/matrix condition of composites; for instance, studying the interface with different fibre treatments/sizing. SEM analysis allowed visualising the interface condition as well as the matrix cracks and surface condition after water absorption.

REFERENCES

[1] Takeda SI, Tsukada T, Sugimoto S, Iwahori Y. Monitoring of water absorption in CFRP laminates using embedded fiber Bragg grating sensors. Compos Part A Appl Sci Manuf 2014;61:163–71. doi:10.1016/j.compositesa.2014.02.018.

[2] Xu L, Huang Y, Zhao C, Ha SK. Progressive failure prediction of woven fabric composites using a multi-scale approach. Int J Damage Mech 2018;27:97–119.

[3] Meredith J, Bilson E, Powe R, Collings E, Kirwan K. A performance versus cost analysis of prepreg carbon fibre epoxy energy absorption structures. Compos Struct 2015;124:206–13.

[4] Baley C, Davies P, Grohens Y, Dolto G. Application of Interlaminar Tests to Marine

Composites. A Literature Review. Appl Compos Mater 2004;11:99–126. doi:10.1023/B:ACMA.0000012902.93986.bf.

[5] Society for Non-Destructive Inspect TJ, editor. Practical Acoustic Emission Testing. Tokyo: Springer Japan; 2016. doi:10.1007/978-4-431-55072-3.

[6] Pérez-Pacheco E, Cauich-Cupul JI, Valadez-González A, Herrera-Franco PJ. Effect of moisture absorption on the mechanical behavior of carbon fiber/epoxy matrix composites. J Mater Sci 2013;48:1873–82. doi:10.1007/s10853-012-6947-4.

[7] Liu PF, Yang J, Peng XQ. Delamination analysis of carbon fiber composites under hygrothermal environment using acoustic emission. J Compos Mater 2017;51:1557–71. doi:10.1177/0021998316661043.

[8] Physical Acoustics Corporation. PCI-2 Baed AE System. 2004.

[9] Imetrum Limited. Video Gauge User Manual - Version 5.0.1. 2016.

[10] ASTM D3171. Standard Test Methods for Constituent Content of Composite Materials. Am Soc Test Mater 2015.

[11] ASTM D 5229. Standard Test Method for Moisture Absorption Properties and Equilibrium Conditioning of Polymer Matrix Composite Materials. Am Soc Test Mater 2014.

[12] ASTM D2344. Standard Test Method for Short-Beam Strength of Polymer Matrix Composite Materials and Their Laminates. Am Soc Test Mater 2016.